J Mater Sci (2010) 45:1930–1936
DOI 10.1007/s10853-009-4182-4

Biomimetic synthesis of needle-like nano-hydroxyapatite templated by double-hydrophilic block copolymer

Xiang Yao · Hongwei Yao · Guoying Li · Yuanting Li

Received: 9 October 2009 / Accepted: 28 December 2009 / Published online: 14 January 2010

Abstract Double-hydrophilic block copolymer (DHBC) poly-(vinylpyrrolidone)-b-poly(vinylpyrrolidone-alt-maleic anhydride)-b-poly-(vinylpyrrolidone) (PVP-b-P(NVP-alt-MAn)-b-PVP) was synthesised as the biomimetic template for the hydroxyapatite (HAP) nanocrystal synthesis. Needle-like HAP nanocrystals can be formed in the presence of PVP_{108}-$P(NVP\text{-}MAn)_{28}$-PVP_{108}. Comparing to the HAP nanocrystals formed in the presence of poly-(vinylpyrrolidone) (PVP) homopolymer, the HAP nanocrystal formed with DHBC is more stable and never precipitate in water after preparation. The crystallization process and the morphology of the final nano-HAP crystal can be controlled by adjusting DHBC molecular structure.

Introduction

Hydroxyapatite (HAP) is the basic component of the natural bone. In the bone formation process, the HAP mineralization is controlled by collagen which is a special protein containing both ionic group which can interact with HAP and dispersive group which may stabilize HAP in the physiological environment [1, 2]. On the other hand, the dental structure is also composed of HAP which is in the needle-like shape and formed under control of proteins [3]. Nearly all of the biological mineralization process is a crystallization process controlled by the organic component [4]. Recently, much attention has been focused on the biomimetic mineralization process because this kind of process may lead to the fabrication of novel materials which cannot be produced by conventional method [5–9]. Cui et al. [10]. reported the mineralization of nano-HAP on self-assembled collagen, the formed nanocomposite has the similar structure and biocompatibility like the natural bone. Tang et al. [11] reported the fabrication of nano-HAP under the control of amino acids and found that both bone-mimetic plate-like and dental-mimetic rod-like nano-HAP can be produced under control of different amino acids. Recently, Lu et al. [12] reported that HAP nanorods can be synthesized in the presence of PVP homopolymer. This method makes it possible to control nano-HAP mineralization by purely synthetic polymer rather than natural biomacromolecules. Since the synthetic polymer has relatively low cost and can be more easily designed, nano-HAP synthesized by this method has great potential usefulness in many applications.

However, the HAP nanocrystals synthesized in the presence of PVP are not stable and easily precipitate in water after preparation because of the relatively weak interaction between PVP and HAP nanocrystal surface. Besides, PVP homopolymer is too simple compared to the biomacromolecule such as protein, the function of protein such as collagen in biomineralization cannot be fully imitated by it. All of the drawbacks hinder further application of this method. Double-hydrophilic block copolymer (DHBC) has already been used as biomimetic template for the organic–inorganic nanocomposite formations [13, 14]. This kind of copolymer usually contains an ionic segment such as the PAA and a nonionic water soluble segment such as PEG [15]. In the biomimetic templating process, the ionic segment acts as the combining part which hold the

X. Yao · Y. Li
Department of Chemical Engineering, Tsinghua University, 100084 Beijing, People's Republic of China

H. Yao (✉) · G. Li
Department of Polymer Science and Engineering, Qingdao University, 266071 Qingdao, People's Republic of China
e-mail: yaohwqd@qdu.edu.cn

inorganic component and the nonionic segment acts as the stabilization part. The final nanostructure formation is greatly dependant on the molecular structure of the DHBC [16–19].

In the present work, we report a novel method for the biomimetic HAP mineralization process. The DHBC PVP-b-P(NVP-alt-MAn)-b-PVP was synthesized through reversible addition fragmentation chain transfer (RAFT) polymerization. And then it was chosen as the template for the needle-like nano-HAP synthesis. The COO^- on the middle block acts as the combining segment of HAP and the PVP side chain acts as the stabilization segment which stabilizes the formed nano-HAP in water. The crystallization mechanism of HAP nanocrystals in the presence of PVP-b-P(NVP-alt-MAn)-b-PVP has been discussed.

Experimental section

Material

All solvents were dried using standard procedures. N-vinylpyrrolidone (NVP) were purchased from Aldrich and purified by distillation under reduced pressure. 2,2-Azobis (isobutyronitrile) (AIBN) was recrystallized from ethanol. Maleic anhydride (MAn) (AR grade, Beijing Yili Chemical Agent Co.), tetrahydrofuran (THF) (AR grade, Shanghai Sihaowei Chemical Engineering Co.), N-heptane, toluene, ammonia solution (AR grade, 25%), calcium hydroxide ($Ca(OH)_2$), phosphoric acid (H_3PO_4) (Shanghai Senni Chemical Engineering Co.) were used without further purification. Dibenzyl trithiocarbonate (DBTTC), synthesized according to literature [20].

RAFT polymerization of PVP macro-CTA

The RAFT polymerization of PVP was conducted in a sealed ampule. The chain transfer agent (CTA) DBTTC (0.232 g, 1 mmol), NVP (40 g, 0.38 mol) and AIBN (0.044 g, 0.276 mmol) were charged into the glass ampule containing 40 g THF. The mixture was degassed through three freeze–thaw cycles. The ampule was then sealed under vacuum and kept in an oil bath at 70 °C to conduct the polymerization. After 5 h, the ampule was put into liquid nitrogen to stop the polymerization. The mixture was precipitated in N-heptane of 15 times excess. This precipitation procedure was repeated 3 times and dried under vacuum. The resulted yellow powder was PVP and stored to be used as the macro-CTA. ^{1}H NMR ($CDCl_3$ 600 MHz): δ 1.3113 (m, 2H), 1.6297 (s, 2H), 1.8873 (t, 2H), 2.0671 (s, 2H), 2.8940 (s, 2H), 3.1574 (d, 2H), 3.3555 (s, 2H), 3.5662 (s, 3H), 3.7357 (s, 3H), 6.2403 (s, 2H), 7.1691 (d, H, aromatic), 7.2504 (s, H, aromatic).

Synthesis of PVP-b-P(NVP-alt-MAn)-b-PVP

The RAFT polymerization of PVP-b-P(NVP-alt-MAn)-b-PVP was conducted in a sealed ampule. In a typical run, NVP (1.5 g, 0.014 mol), MAn (1.4 g, 0.014 mol), and AIBN (0.026 mg, 0.16 mmol) were charged into the glass ampule containing 30 g THF together with 12 g PVP macro-CTA. The mixture was degassed through three freeze–thaw cycles. The ampule was then sealed under vacuum and kept in an oil bath at 60 °C to conduct the polymerization. After 20 h, the mixture was precipitated in toluene of 15 times excess. This precipitation procedure was repeated 3 times and dried under vacuum. The resulted yellow powder was PVP-b-P(NVP-alt-MAn)-b-PVP. The number of the repeat units of respective blocks was calculated from the NMR data. To determine the anhydride content within the obtained three block copolymer, PVP-b-P(NVP-alt-MAn)-b-PVP (1.5 g) was dissolved into 40 mL butanone. After the sample was dissolved, 6 mL pyridine and 6 mL water were added under stirring. The stirring was continued for another 4 h and then the sample was titrated by KOH–ethanol solution using Thymol blue (1%) as the indicator. ^{1}H NMR ($CDCl_3$ 600 MHz): δ 1.3376 (m, 2H), 1.5483 (s, 2H), 1.6319 (s, 2H), 1.8908 (t, 2H), 2.0534 (d, 2H), 2.2996 (s, 2H), 2.5023 (s, 2H), 2.8906 (s, 2H), 3.0761 (s, 2H), 3.1585 (s, 2H), 3.4036 (m, 2H), 3.5513 (s, 3H), 3.7369 (s, 3H), 6.2690 (s, 2H), 7.1691 (d, H, aromatic), 7.2504 (s, H, aromatic).

HAP mineralization templated by double-hydrophilic block copolymer

PVP_{108}-$P(NVP\text{-}MAn)_{28}$-PVP_{108} (1 g) was dissolved into double distilled water at 60 °C. $Ca(OH)_2$ (1.5 g, 0.02 mol) was added and stirred for 1 h. Aqueous solution of 85% H_3PO_4 (1.38 g, 0.012 mol) was added dropwise within 30 min. After completion of the addition, the suspension was adjusted to pH 8.5–9 using 10% ammonia solution and reacted for another 1 h at 60 °C. The same procedure was carried out once everyday for many times and finally reacted for 18 h at 60 °C. The product was purified by several washes with double distilled water and centrifugation at 6000 rpm for 20 min. The final product was obtained by freeze-drying for 48 h.

Characterization

Nuclear magnetic resonance (NMR) spectroscopy

All ^{1}H NMR spectra were recorded using a Bruker 600 MHz spectrometer. Samples were analyzed in $CDCl_3$.

FTIR

The FTIR spectra were recorded on a Nicolet Nexus 670 instrument, measured in transmission mode using the KBr self-supported pellet technique.

Gel permeation chromatography (GPC)

GPC analysis was carried out with a LC98R1 system equipped with KF-802, KF-803, KF-804 columns and a Shodex R1-71 refractive index detector. THF was used as eluent at a flow rate of 1 mL/min at 35 °C. Mono-dispersed polystyrene standards were used to obtain a calibration curve.

Transmission electron microscopy (TEM)

TEM, high-resolution transmission electron microscopy (HRTEM), and selected-area electron diffraction (SAED) studies were performed on a FEI Tecnai G2 20 S-TWIN transmission electron microscope operated at 200 kV.

X-ray diffraction (XRD)

X-ray diffraction patterns were measured in a Phlip X Pert-MPD equipment using Cu Kα radiation.

TGA

The thermal properties were analyzed using TA instrument TGA 2950 at a heating rate of 10 °C/min.

Discussion

The DHBC PVP-b-P(NVP-alt-MAn)-b-PVP was synthesized through RAFT living polymerization. The general procedure for the synthesis process can be illustrated by Scheme 1. Because the chain transfer reaction was carried out in the middle of the CTA, the PVP side block was firstly synthesized. The NVP and MAn monomers were then added into the reaction and formed the middle block of the copolymer through the alternative polymerization. GPC results show that each of the synthesized PVP block has the number average molecular weight (M_n) of 23976 and a narrow molecular weight distribution (PDI) of 1.13. Two kinds of block copolymer with different middle block have been synthesized. The M_n and PDI of the two kinds of block copolymer are $M_n = 29828$, PDI = 1.22 for PVP_{108}-$P(NVP\text{-}MAn)_{28}$-PVP_{108} and $M_n = 35471$, PDI = 1.26 for PVP_{108}-$P(NVP\text{-}MAn)_{55}$-PVP_{108}, respectively. Because of the double hydrophilic property of the two blocks, this type of block copolymer cannot form micelle in water without the addition of other components.

TEM image (Fig. 1a) shows the morphology of the prepared needle-like HAP nanocrystals in the presence of the PVP_{108}-$P(NVP\text{-}MAn)_{28}$-PVP_{108}. The HRTEM (Fig. 1b) shows a typical apatite crystalline structure. The lattice fringes with a spacing of 0.32 nm is in agreement with the spacing of the (002) plane of HAP while the 0.79 nm is the spacing of (100) plane. The XRD pattern of the above sample is shown in Fig. 2. The typical crystalline peaks of HAP at $2\theta = 25.76°$, 28.16°, 29.1°, 31.86°, 33°, 34.06°, and 40.04° can be clearly seen with some deviation due to the presence of organic component.

TGA data (Fig. 3) show that the organic/inorganic content ratio is about 4/6 indicating that most of the block copolymer is adsorbed on the HAP nanocrystal after preparation. This organic content stabilizes the HAP nanocrystal preventing it from precipitation. As shown in Fig. 4, the HAP dispersion formed after 1, 3, 8, 11, 13 days never aggregates after its formation. Experiments have confirmed that only the DHBC PVP-b-P(NVP-alt-MAn)-b-PVP may obtain the needle-like HAP nanocrystal without precipitation after a long time. PVP has been reported as an efficient capping agent for the synthesis of HAP nanocrystal and the formed HAP may exhibit the needle-like morphology, whereas the product is apt to aggregate together after a few hours. It has been revealed that the N–C=O group on PVP may form hydrogen bond with OH

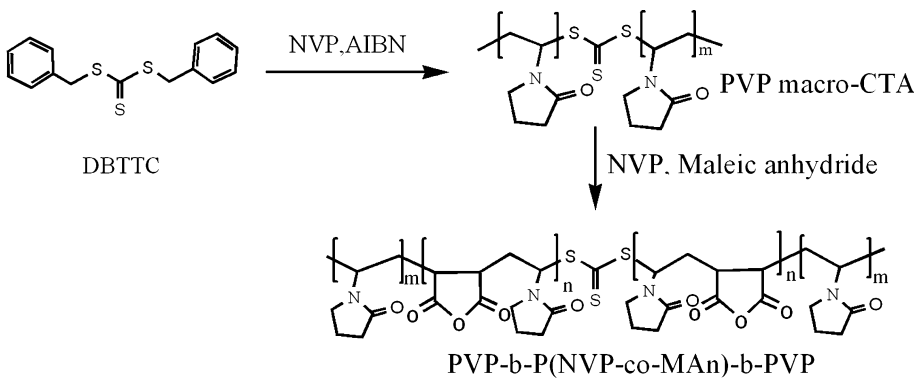

Scheme 1 Synthesis of double-hydrophilic block copolymer PVP-b-P(NVP-alt-MAn)-b-PVP

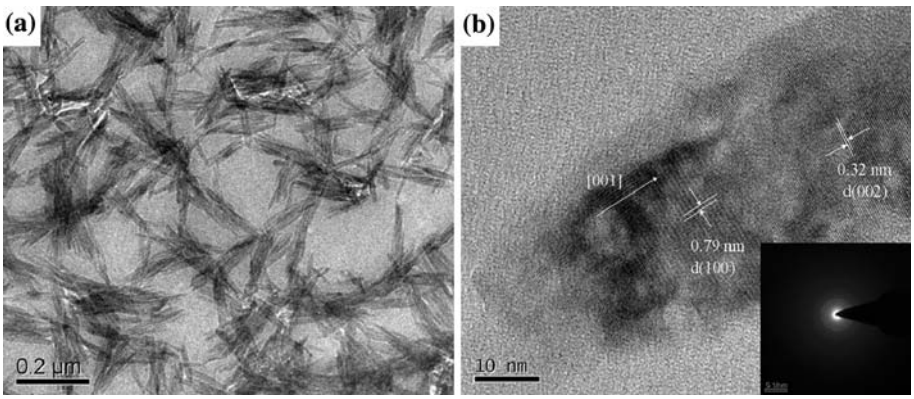

Fig. 1 **a** TEM, **b** HRTEM and SAED of needle-like HAP nanocrystals templated by PVP_{108}-$P(NVP\text{-}MAn)_{28}$-PVP_{108}

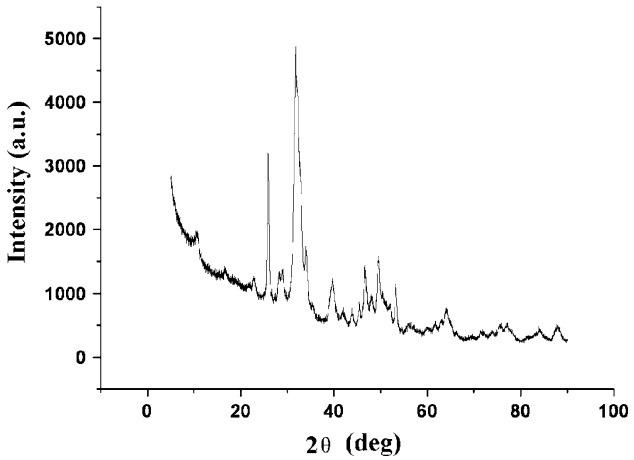

Fig. 2 XRD pattern of needle-like HAP nanocrystals templated by PVP_{108}-$P(NVP\text{-}MAn)_{28}$-PVP_{108}

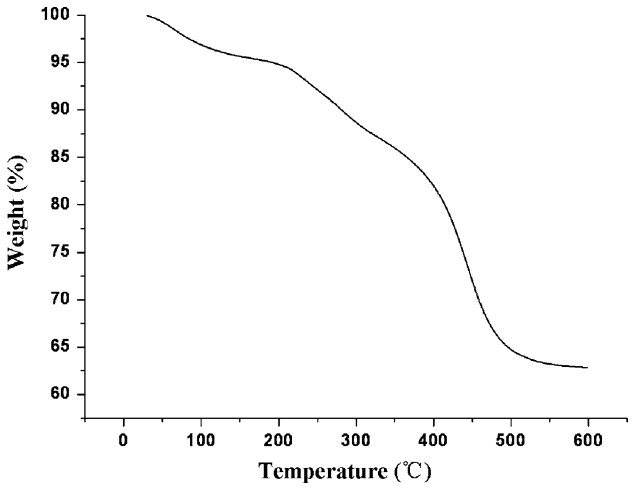

Fig. 3 TGA of needle-like HAP nanocrystals showing changes in wt%

group on the crystal surface of HAP nanocrystals other than *c* axis [10]. So the HAP nanocrystal will only grow along the *c* axis. The resulted HAP exhibits a rod-like or

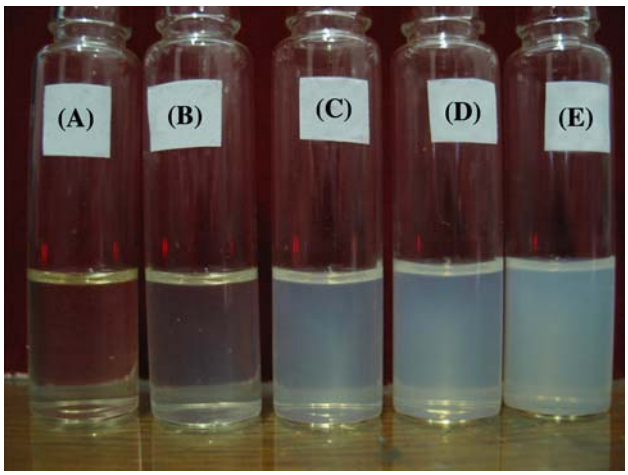

Fig. 4 Picture of needle-like HAP nanocrystals templated by PVP_{108}-$P(NVP\text{-}MAn)_{28}$-PVP_{108} after the preparation of (from left to right bottles): 1 day (*A*), 2 days (*B*), 8 days (*C*), 10 days (*D*), 13 days (*E*)

needle-like morphology. However, because the PVP only form hydrogen bond with HAP, it is easily depart from the HAP nanocrystal and the HAP without the PVP protection is easily aggregate together in water. The aggregated HAP is not stable and is apt to precipitate after a few hours. On the other hand, the HAP nanocrystal can also be stabilized by COO^- through ionic bond with Ca^{2+}. Comparing with hydrogen bond, the ionic bond between COO^- and Ca^{2+} is more stable in water. However, the polymer contained only COO^- such as the polyacrylic acid may form aggregation with HAP because the Ca^{2+}-associated PAA is insolvable in water. Only the HAP formed in the presence of DHBC PVP-b-P(NVP-alt-MAn)-b-PVP may keep its solubility in water solution. In this case, HAP is stabilized by both COO^- and PVP side chain. The alternative MAn and NVP monomer unit in the middle block may form both ionic and hydrogen bond with HAP crystal surface. This strong interaction prevents the detachment of the DHBC from HAP nanocrystal. Because the presence of PVP in the side block, the formed HAP crystal may keep its solubility in water. Because the COO^- and PVP will only adsorb on the

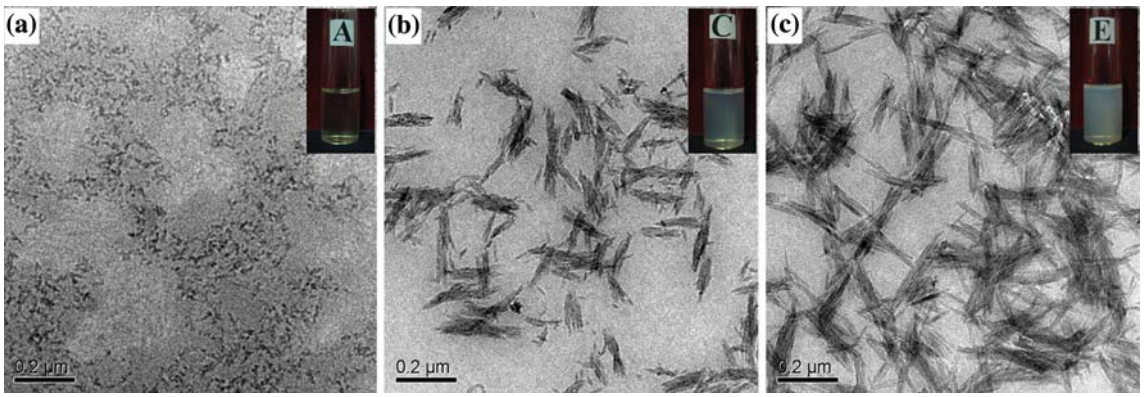

Fig. 5 TEM images of HAP nanocrystals templated by PVP_{108}-$P(NVP\text{-}MAn)_{28}$-PVP_{108} after the preparation of: **a** 1 day, **b** 8 days, **c** 13 days

HAP surface other than *c* axis, the formed HAP nanocrystal in the presence of PVP-b-P(NVP-alt-MAn)-b-PVP may exhibit a needle-like morphology like the case of PVP. To have a better understand on the mechanism of the HAP nanocrystal formation process, the product after 1, 8, 13 days were observed by TEM (Fig. 5). In the presence of Pnm, HAP may start to nucleate and form amorphous HAP nanoparticles (Fig. 5a). After 8 days growth, the bundle of needle-like HAP nanocrystal may form (Fig. 5b). However, at this time the size of HAP nanocrystal is not uniform, some short nanocrystal is mixed together with the longer ones. After 13 days growth, both of the short and long nanocrystals form a needle-like morphology (Fig. 5c). DLS data (Fig. 6) support the TEM observation. At the beginning of the HAP formation, the size of the nanocrystal is 10 nm and has a narrow distribution. When the HAP nanocrystals grow for 8 days, nanocrystals with small and large size coexist together. After 13 days growth, the sizes

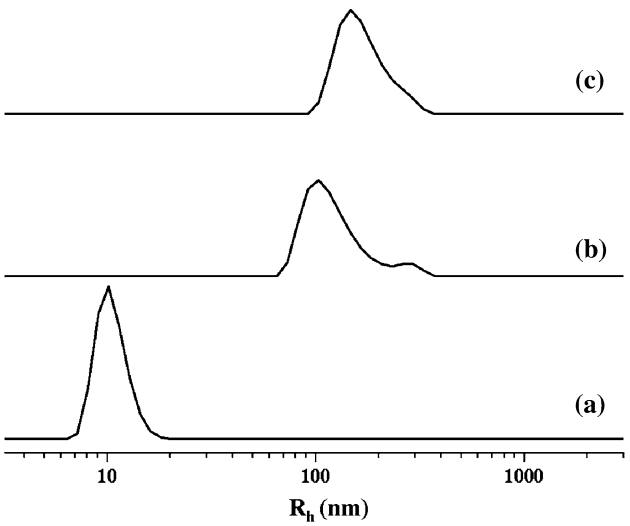

Fig. 6 Dynamic light scattering results for size growth of HAP nanocrystals templated by PVP_{108}-$P(NVP\text{-}MAn)_{28}$-PVP_{108} at different preparation times: (*a*) 1 day, (*b*) 8 days, (*c*) 13 days

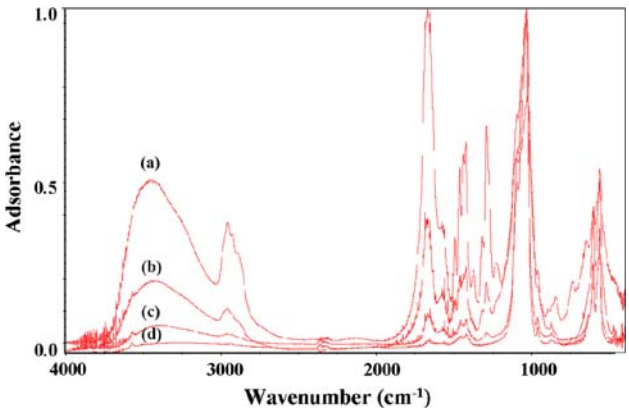

Fig. 7 FTIR spectra of HAP nanocrystals templated by PVP_{108}-$P(NVP\text{-}MAn)_{28}$-PVP_{108} obtained for (*a*) 1 day, (*b*) 8 days, (*c*) 13 days, (*d*) HAP nanocrystals formed without template

of the nanocrystal become a single narrow distribution again with the average size of 150 nm which is identical with the TEM observation.

Figure 7 shows the FTIR of the prepared HAP nanocrystal with (Fig. 7a–c) and without (Fig. 7d) PVP-b-P(NVP-alt-MAn)-b-PVP. The 3568 cm^{-1} stretching band and 630 cm^{-1} bending band can be attributed to the interaction of N–C=O group in PVP with OH on the surface of HAP nanocrystals. These two bands did not disappeared after 13 days growth of HAP indicating that the organic DHBC never departed with HAP nanocrystals. This result confirmed the former discussion. The bands at 1096, 1032, 962, 603, and 564 cm^{-1} are attributed to PO_4^{3-} ions. These bands together with the former two OH bands confirm the formation of HAP nanocrystals. With the addition of HAP precursor and the growth of HAP nanocrystals, the intensity of HAP adsorption gradually dominates indicating that the content of inorganic component increasing.

To test whether the molecular structure of the DHBC has an influence on the HAP nanocrystal formation, two kinds of PVP-P(NVP-MAn)-PVP with different middle

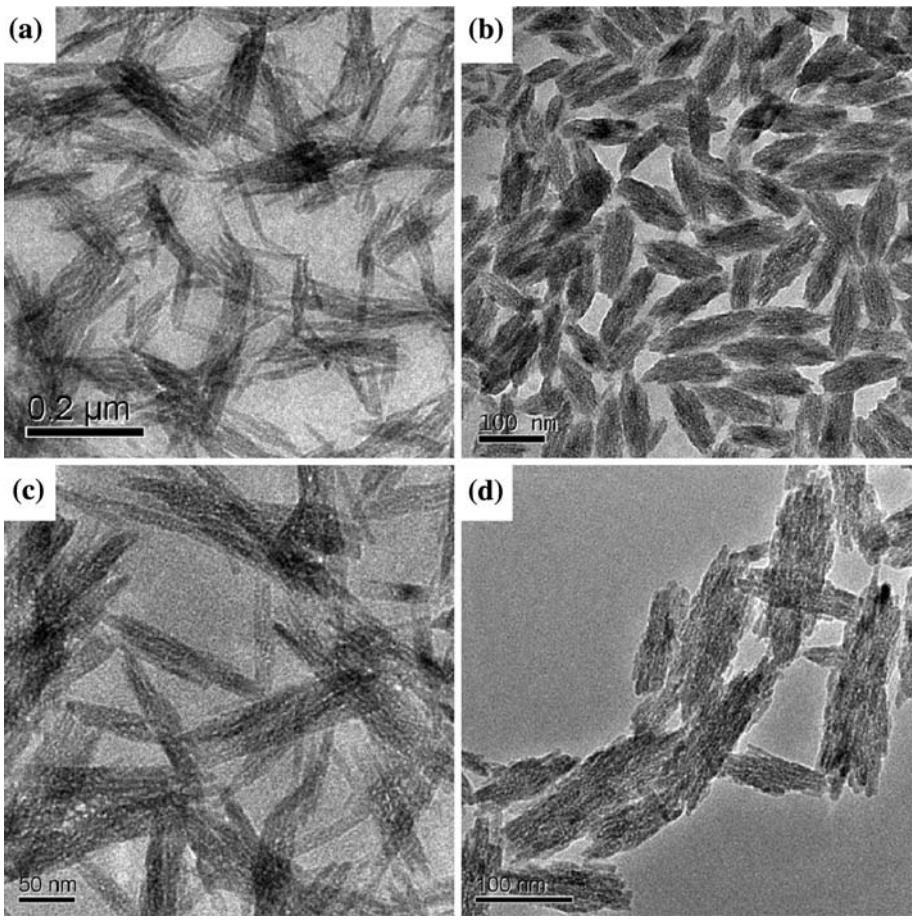

Fig. 8 TEM images of HAP nanocrystals templated by **a** PVP_{108}-$P(NVP\text{-}MAn)_{28}$-PVP_{108}; **b** PVP_{108}-$P(NVP\text{-}MAn)_{55}$-PVP_{108}; **c** magnified image of **a**; **d** magnified image of **b**

block length but the same side block length PVP_{108}-$P(NVP\text{-}MAn)_{28}$-PVP_{108} and PVP_{108}-$P(NVP\text{-}MAn)_{55}$-PVP_{108} has been synthesized as formerly discussed. As shown in Fig. 8, the HAP formed in the presence of PVP_{108}-$P(NVP\text{-}MAn)_{28}$-PVP_{108} has a needle-like morphology while that formed in the presence of PVP_{108}-$P(NVP\text{-}MAn)_{55}$-PVP_{108} has a bundle-like shape. Since the main difference between the two kinds of block copolymer is their middle block content, the MAn and NVP alternative unit must take an important role for the control of the nanocrystal shape. As reported by Zhang et al. [10], after the nucleation and the formation of the initial particles, the growth of HAP nanocrystal is corporately controlled by Ostwald ripening and oriented attachment. In the presence of PVP_{108}-$P(NVP\text{-}MAn)_{28}$-PVP_{108}, the $P(NVP\text{-}MAn)_{28}$ middle block adsorbs onto the surface of HAP during crystal growth and prevents the crystal growth other than *c* axis. Because of the presence of relatively longer PVP side chain, the Ostwald ripening growth of the crystal has been hindered and the oriented attachment dominates the HAP crystal growth which results in the formation of needle-like nanocrystals with high respect ratio (Fig. 8a, c). In the case of the PVP_{108}-$P(NVP\text{-}MAn)_{55}$-PVP_{108}, the relatively longer middle block enhanced the lateral interaction between the initial particles while the relatively shorter PVP side chain cannot efficiently prevent the Ostwald ripening. Although the oriented attachment still has its effect, the Ostwald ripening becomes dominate in this case which results in the formation of bundle-like aggregates of the small nanocrystals (Fig. 8b, d).

Conclusion

We described a novel biomimetic method for the synthesis of needle-like HAP nanocrystals templated by DHBCs. Needle-like morphology of HAP nanocrystals can be obtained in the presence of PVP_{108}-$P(NVP\text{-}MAn)_{28}$-PVP_{108}. The prepared nanocomposite has excellent dispersive property and it will never precipitate after preparation. The crystallization process of the HAP nanocrystal can be controlled by both preparation time and molecular structure of DHBCs. HAP nanocrystals formed by this method exhibit different size

and morphology at different preparation times. The HAP formed in the presence of PVP_{108}-$P(NVP\text{-}MAn)_{28}$-PVP_{108} has a needle-like morphology while that formed in the presence of PVP_{108}-$P(NVP\text{-}MAn)_{55}$-PVP_{108} has a bundle-like shape because of the different crystallization mechanisms in the presence of different DHBCs.

References

1. Cai YR, Tang RK (2008) J Mater Chem 18:3775
2. Vallet-Regi M, Gonza′lez-Calbet JM (2004) Prog Solid State Chem 32:1
3. Chen H, Chen Y, Orr BG, Banaszak-Holl M, Majoros I, Clarkson BH (2004) Langmuir 20:4168
4. Sergey V, Dorozhkin SV (2007) J Mater Sci 42:1061. doi: 10.1007/s10853-006-1467-8
5. Boduch-Lee KA, Chapman T, Petricca SE, Marra KG, Kumta P (2004) Macromolecules 37:8959
6. Kaneko T, Ogomi D, Mitsugi R, Serizawa T, Akashi M (2004) Chem Mater 16:5596
7. Malkaj P, Pierri E, Dalas E (2005) J Mater Sci Mater Med 16:733
8. Song J, Saiz E, Bertozzi CR (2003) J Am Chem Soc 125:1236
9. Song J, Malathong V, Bertozzi CR (2005) J Am Chem Soc 127:3366
10. Zhang W, Liao SS, Cui FZ (2003) Chem Mater 15:3221
11. Pan HH, Tao JH, Xu XR, Tang RK (2007) Langmuir 23:8972
12. Zhang YJ, Lu J (2008) J Cryst Growth Des 8:2101
13. Colfen H (2001) Macromol Rapid Commun 22:219
14. Sedlak M, Antonietti M, Colfen H (1998) Macromol Chem Phys 199:247
15. Tjandra W, Yao J, Ravi P, Kam C, Tam KC, Alamsjah A (2005) Chem Mater 17:4865
16. Colfen H, Antonietti M (1998) Langmuir 14:582
17. Qi L, Colfen H, Antonietti M (2000) Angew Chem Int Ed 39:604
18. Yu SH, Antonietti M, Colfen H, Giersig M (2002) Angew Chem Int Ed 41:2356
19. Yu SH, Antonietti M, Colfen H, Hartmann J (2003) Nano Lett 3:379
20. Mayadunne RTA, Rizzardo E, Chiefari J (2000) Macromolecules 33:243